A 1-year long delta O-18 record of water vapor in Niamey (Niger) reveals insightful atmospheric processes at different timescales

Guillaume Tremoy, Francoise Vimeux, Salla Mayaki, Ide Souley, Olivier Cattani, Camille Risi, Guillaume Favreau, Monique Oi

A 1-year long $\delta^{18}O$ record of water vapor in Niamey (Niger) reveals insightful atmospheric processes at different timescales

Guillaume Tremoy,[1] Françoise Vimeux,[1,2] Salla Mayaki,[3] Ide Souley,[3] Olivier Cattani,[1] Camille Risi,[4] Guillaume Favreau,[2] and Monique Oi[2]

Received 20 February 2012; revised 23 March 2012; accepted 26 March 2012; published 24 April 2012.

[1] We present a 1-year long representative $\delta^{18}O$ record of water vapor ($\delta^{18}O_v$) in Niamey (Niger) using the Wavelength Scanned-Cavity Ring Down Spectroscopy (WS-CRDS). We explore how local and regional atmospheric processes influence $\delta^{18}O_v$ variability from seasonal to diurnal scale. At seasonal scale, $\delta^{18}O_v$ exhibits a W-shape, associated with the increase of regional convective activity during the monsoon and the intensification of large scale subsidence North of Niamey during the dry season. During the monsoon season, $\delta^{18}O_v$ records a broad range of intra-seasonal modes in the 25–40-day and 15–25-day bands that could be related to the well-known modes of the West African Monsoon (WAM). Strong $\delta^{18}O_v$ modulations are also seen at the synoptic scale (5–9 days) during winter, driven by tropical-extra-tropical teleconnections through the propagation of a baroclinic wave train-like structure and intrusion of air originating from higher altitude and latitude. $\delta^{18}O_v$ also reveals a significant diurnal cycle, which reflects mixing process between the boundary layer and the free atmosphere during the dry season, and records the propagation of density currents associated with meso-scale convective systems during the monsoon season. **Citation:** Tremoy, G., F. Vimeux, S. Mayaki, I. Souley, O. Cattani, C. Risi, G. Favreau, and M. Oi (2012), A 1-year long $\delta^{18}O$ record of water vapor in Niamey (Niger) reveals insightful atmospheric processes at different timescales, *Geophys. Res. Lett.*, *39*, L08805, doi:10.1029/2012GL051298.

1. Introduction

[2] Although crucial progress have been made in understanding atmospheric processes over West Africa [*Lafore et al.*, 2010], several questions prevail. Quantification of the relative effect of large-scale circulation, convection processes such as rain evaporation, and continental recycling on the atmospheric water cycle budget is not perfectly known from diurnal to seasonal scales [*Risi et al.*, 2010a]. Teleconnections between the WAM and extra-tropical modes of intra-seasonal variability are not well understood [*Janicot et al.*, 2010; *Chauvin et al.*, 2010].

[3] The isotopic composition of Niger precipitation ($\delta^{18}O_p$) has been recorded during the 2006 Monsoon season [*Risi et al.*, 2008a, 2010b]. Those latter studies showed the potential of water stable isotopes to further examine convective processes and organization. However, to further disentangle the various atmospheric controls on $\delta^{18}O_p$, to better document the evolution of moistening processes by rain evaporation, to better examine mesoscale subsidence in convective systems, to better know the origin of water vapor or to better evaluate convective processes in climate models, the isotopic composition of water vapor ($\delta^{18}O_v$) is needed.

[4] We extend here the previous observations through an original continuous 1-year long representative $\delta^{18}O_v$ (accuracy of ±0.25‰) [*Tremoy et al.*, 2011] recorded in Niamey (Niger), at the Institut des RadioIsotopes (IRI, 13.31°N 2.06°E, 218 m.a.s.l) using a Picarro laser instrument (L1102-i model) [*Gupta et al.*, 2009] from 2 July 2010 to 12 May 2011. δD_v was also recorded but we focus here on $\delta^{18}O_v$. Precipitation was also collected on an event-based resolution and analyzed with an accuracy of ±0.05‰ for $\delta^{18}O_p$. Our paper explores the $\delta^{18}O_v$-$\delta^{18}O_p$ relationship, discusses the potential of $\delta^{18}O_v$ at the seasonal, intra-seasonal and diurnal timescales and examines the comparison between our observations and a nudged LMZ-iso simulation [*Risi et al.*, 2010c].

2. Representativeness of Surface Data

[5] We present here near surface measurements (~8 m above the ground) that may lead to important limitations. However, we argue that near-surface $\delta^{18}O_v$ can capture atmospheric processes. First, *Risi et al.* [2008b] clearly showed that water vapor in the subcloud layer is highly influenced by processes such as reevaporation in convective downdrafts. Second, by comparing observed $\delta^{18}O_v$ and $\delta^{18}O_p$ from July to October 2010 (Figure 1 and see next section), we show that surface water vapor variations are not disconnected from the water vapor from which precipitation forms in altitude ($r^2 = 0.66$, n = 39). Third, in the LMDZ-iso simulation described by *Risi et al.* [2010c], the correlation between $\delta^{18}O_v$ in Niamey grid point at 1000 hPa and the same values at 850 hPa is of 0.86, and decreases to 0.62 (0.33) at 750 hPa (650 hPa) over the whole period of simulation (January 2010–April 2011). In the same simulation, the correlation between $\delta^{18}O_v$ in Niamey grid point and adjacent grid points is higher than 0.6 all over the year. The LMDZ-iso simulation thus suggests that the very local surface near observation might be useful as a proxy for boundary layer processes.

3. Is Water Vapor in Isotopic Equilibrium With Precipitation?

[6] In this section, we explore to what extent $\delta^{18}O_v$ and $\delta^{18}O_p$ are far from the theoretically isotopic equilibrium

[1]Laboratoire des Sciences du Climat et de l'Environnement, UMR 8212, Institut Pierre Simon Laplace, CEA-CNRS-UVSQ, Gif-sur-Yvette, France.
[2]Laboratoire HydroSciences Montpellier, UMR 5569, Institut de Recherche pour le Développement, CNRS-IRD-UM1-UM2, Montpellier, France.
[3]Institut des RadioIsotopes, Université Abdou Moumouni de Niamey, Niamey, Niger.
[4]Laboratoire de Météorologie Dynamique, Institut Pierre Simon Laplace, UPMC-CNRS, Paris, France.

0094-8276/12/2012GL051298

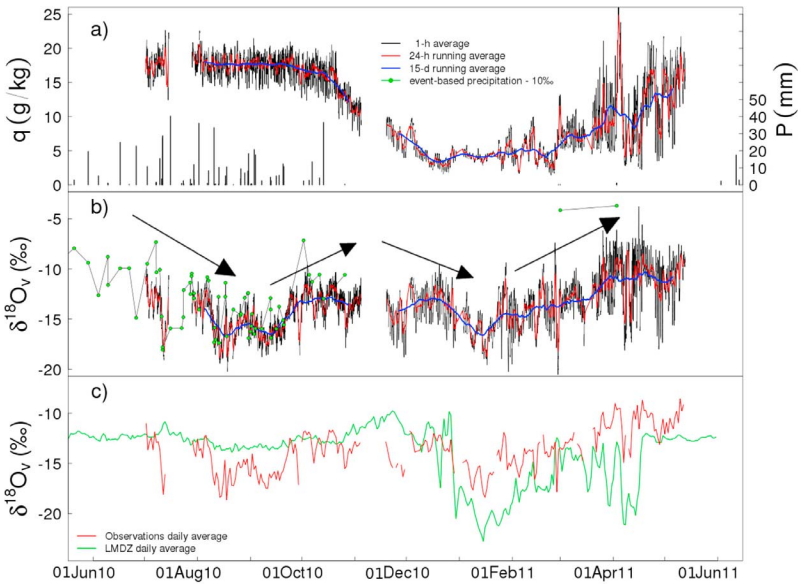

Figure 1. Temporal evolution from June 2010 to May 2011 of (a) Specific humidity q (g/kg) along with event-based rainfall amount P (mm). From 23 April to 26 October 2010, 66 rain events were collected (total amount of 523.8 mm, precipitation varied from 0.1 mm to 40.3 mm); (b) $\delta^{18}O_v$ (‰): black, red and blue lines are hourly averages, 24-h and 15-days running averages respectively. Intense power cuts (from 15 to 28 July 2010) and maintenance period (from 5 to 18 Nov 2010), where a new automated calibration system was set up, are responsible for the 2 major gaps. Event-based ($\delta^{18}O_p - 10$) (‰) are in green dots; and (c) $\delta^{18}O_v$ (‰) in our observations (red line) and in LMDZ-iso (green dotted line).

($\delta^{18}O_{veq}$) (please see legend of Figure S1 in the auxiliary material for the $\delta^{18}O_{veq}$ calculation from $\delta^{18}O_p$).[1] We find that $\delta^{18}O_v$-$\delta^{18}O_{veq}$ is mostly negative, specifically for the 2 events in April where $\delta^{18}O_v$-$\delta^{18}O_{veq}$ is of −6.4 and −4.9‰ suggesting high evaporative effects. The robust feature (mostly independent of condensation temperature) is the positive linear evolution of $\delta^{18}O_v$-$\delta^{18}O_{veq}$ as a function of relative humidity ($r^2 = 0.54$) showing that as expected, isotopic exchanges are closer to the isotopic equilibrium for high relative humidity (see Figure S1).

4. The $\delta^{18}O_v$ Modes of Variability

4.1. A W-Shape Seasonal $\delta^{18}O_v$ Variation

[7] As expected, q shows a seasonal cycle with the highest (lowest) values (15–20 g/kg) (<10 g/kg) occurring from July to September 2010 (from November 2010 to March 2011) (Figure 1a). By contrast, $\delta^{18}O_v$ exhibits a distinct W-shape seasonal variability (Figure 1b) with a seasonal amplitude of around 6‰. A first $\delta^{18}O_v$ minimum is observed within the monsoon season, from August to September ($m_{Aug–Sept} = -15.45 \pm 1.78$‰) and captures two minimum values in mid-August and mid-September while a second minimum is exhibited within the dry season, in January ($m_{January} = -15.45 \pm 1.94$‰). The $\delta^{18}O_v$ depletion during the summer monsoon reflects the increasing convective activity at the regional scale as expected from the "amount effect" and its consequence on the subsequent vapor [*Dansgaard*, 1964]. Interestingly, this first isotopic minimum is not observed by SCIAMACHY near-surface δD_v space-borne measurements [*Frankenberg et al.*, 2009]. The second isotopic depletion (observed by SCIAMACHY near-surface δD_v although more depleted) can be related to large-scale subsidence originating from the descending Hadley cell, stronger from January to March and transporting depleted air masses from high altitude down to the surface as suggested by *Frankenberg et al.* [2009].

[8] The monsoon retreat (October to November 2010) is characterized by an enrichment of the vapor as the convective activity decreases. Averaged $\delta^{18}O_v$ over Oct.–Nov. is -13.39 ± 1.34‰. The moistening period (April–May) is characterized by a progressive increase of $\delta^{18}O_v$, which could reflect change in moisture source: the monsoon flow propagates northward and the water vapor from the Equatorial band is more enriched than at the latitude of Niamey [*Frankenberg et al.*, 2009, Figure 1a]. Annual $\delta^{18}O_v$ maximum is reached right before the monsoon onset ($m_{May} = -9.59 \pm 1.28$‰; from 1 to 12 May).

4.2. Intra-seasonal Timescales

[9] To determine the dominant intra-seasonal modes of $\delta^{18}O_v$ variability, we performed a wavelet analysis [*Torrence and Compo*, 1998] on the hourly interpolated $\delta^{18}O_v$ data (see Figure S2).

[10] During summer monsoon, a significant signal is seen in the 25–40-day band. Other significant modes (at the 90% confidence level) are detected in the 15–25-day band (only at the beginning of the monsoon in July), and in the 6–12-day band at the beginning (1 to 10 July) and at the end of the monsoon (20 September to 10 October). Fluctuations in the 1–5-day band are also recorded, but with a weaker amplitude. These modes are known to modulate convection in West

[1]Auxiliary materials are available in the HTML. doi:10.1029/2012GL051298.

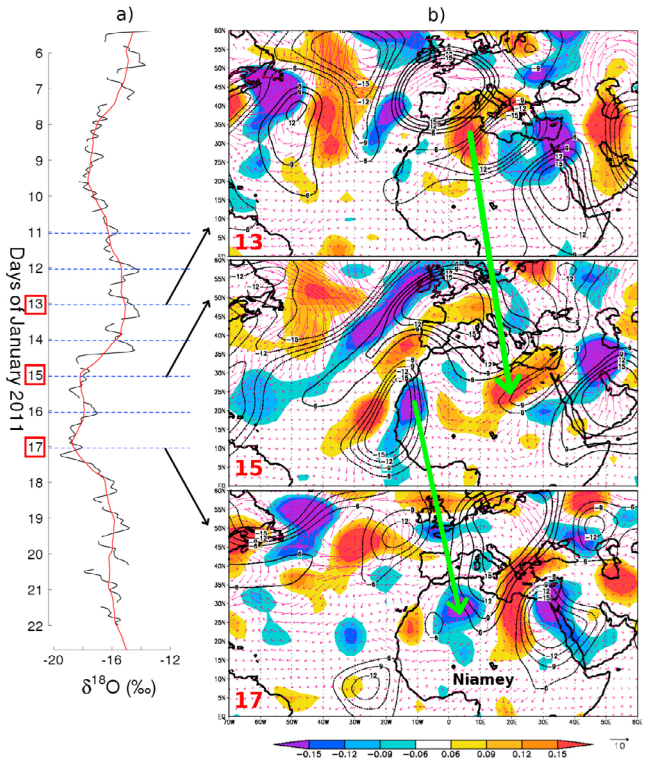

Figure 2. (a) Temporal evolution from 3 to 20 January 2011 (horizontal dotted lines are at 00 UTC) of $\delta^{18}O_v$ (‰). (b) Sequence from 13 to 17 January of daily anomalies (relative to the 3 to 20 January base period) in vertical velocity at 500 hPa (shaded, Pa s^{-1}), 300 hPa stream function (contour, interval is 3.10^6 $m^2.s^{-1}$), and 925 hPa wind (red vectors, a 10 m s^{-1} vector wind is indicated at the bottom right of the figure. Positive (red) vertical velocity indicate region of subsidence, positive stream function (solid contour) indicate upper-tropospheric anticyclonic circulation. Niamey is located at 13.31°N, 2.06°E (black dot). Black arrows link the time-series in Figure 2a and the maps in Figure 2b referring to the same days. Green arrows indicate the eastward displacement of the vertical velocity anomalies.

Africa [*Janicot et al.*, 2010] and may reflect the property of $\delta^{18}O_v$ to integrate convective activity (the stronger the convection, the lower the $\delta^{18}O_v$) both in time and space. Indeed, the correlation between daily $\delta^{18}O_v$ time-series and OLR (Outgoing Longwave Radiation, from the National Oceanic and Atmospheric Administration (NOAA) polar-orbiting satellites [*Liebmann and Smith*, 1996]) averaged over the 9 previous days from July to September 2010 is maximum ($r > 0.6$) Southwest and East of Niamey, suggesting a strong influence of integrated convective activity along the southerly monsoon flow and the westwards propagation of convective systems on $\delta^{18}O_v$ (see Figure S3).

[11] From December to March, $\delta^{18}O_v$ shows strong and significant periodicities at synoptic scales, with a major periodicity around 5–9 days, for example around 16 January (Figure 2a). Figure 2b shows a sequence from 13 to 17 January of the 500 hPa vertical velocity (to inspect the mid-tropospheric subsidence), the 300 hPa stream function (upper tropospheric circulation) and surface winds anomalies (relative to the 3 to 20 January based period). We observe a well-developed baroclinic wave train-like structure consisting of alternating positive and negative vertical velocity anomaly centers following an arch trajectory from the mid-latitude North Atlantic to North Africa across southern Mideast Africa. Prior to the $\delta^{18}O_v$ minimum, subsidence, associated with anticyclonic circulation, is maximum north of Niamey, and southwards surface wind speed increases. As the wave train propagates eastward, $\delta^{18}O_v$ decreases. We also observe a decrease in surface temperature (which exceeds −3°C) that could be related to the southward moisture transport (positive vertical velocity) of cold air from higher latitude at around 30°N (see Figure S4). On 17 January, $\delta^{18}O_v$ increases as subsidence weakens (the vertical velocity anomaly becomes mostly negative over North Africa at the Niamey longitude). Our observations suggest that surface $\delta^{18}O_v$ in Niamey is strongly modulated at synoptic timescale by tropical-extra-tropical teleconnections.

4.3. Variability at the Convective Event Scale

[12] During the monsoon season, no systematic diurnal cycle can be seen: the strongest $\delta^{18}O_v$ variations occur with precipitation events and no diurnal cycle is seen when accounting for non-rainy days only. However, robust features are seen considering the rainy days. In the following, we only consider rain events where P > 5 mm. 16% are associated with an increase in $\delta^{18}O_v$ from the beginning (sometimes before) to the end of the rain event, with a maximum increase of +2.9‰ observed on 17 August 2010. These variations could correspond to strong rain evaporation events and weak subsidence in the unsaturated downdraft (see discussion below). On the contrary, for 84% of rain events, $\delta^{18}O_v$ exhibits a sharp decrease (from ∼−2 to −5‰), most of the time at the beginning of the rain events (Figure 3b), in phase with a surface temperature drop (∼−3 to −10°C). However, $\delta^{18}O_v$ and temperature drops are observed more than 30 min before rain onset in 19% of the depleting events and up to 2 hours before for less that 1% of all events. This $\delta^{18}O_v$ feature (including the possible delay) could reflect the propagation of density currents (cold pools) initiated by rain evaporation in unsaturated downdrafts, and propagating at the bottom of the system through a rear-to-front dry flow induced by meso-scale subsidence in the stratiform zone of the squall line [*Houze et al.*, 1989]. Indeed, the strong droplet reevaporation in the stratiform zone induces an isotopic decrease (increase) of $\delta^{18}O_v$, provided that evaporation rate is low (high) and that relative humidity is high (low) [*Stewart*, 1975; *Bony et al.*, 2008]. Thus, along a squall line, surface $\delta^{18}O_v$ may essentially result from the relative contribution of the dynamics, which bring depleted water vapor from higher altitude by previous condensation process, and the rain evaporation, which tend to enrich or to deplete the water vapor, depending on the relative humidity of the environment and the fraction of remaining droplets in the downdraft [*Risi et al.*, 2010b]. We clearly show in Figure 3c that the $\delta^{18}O_v$ evolution in the course of precipitation event, and also before and after it, is not explained by a basic Rayleigh distillation. We may explain the small increase in q at the end of the precipitation event by reevaporation of droplets leading to remoistening the environment.

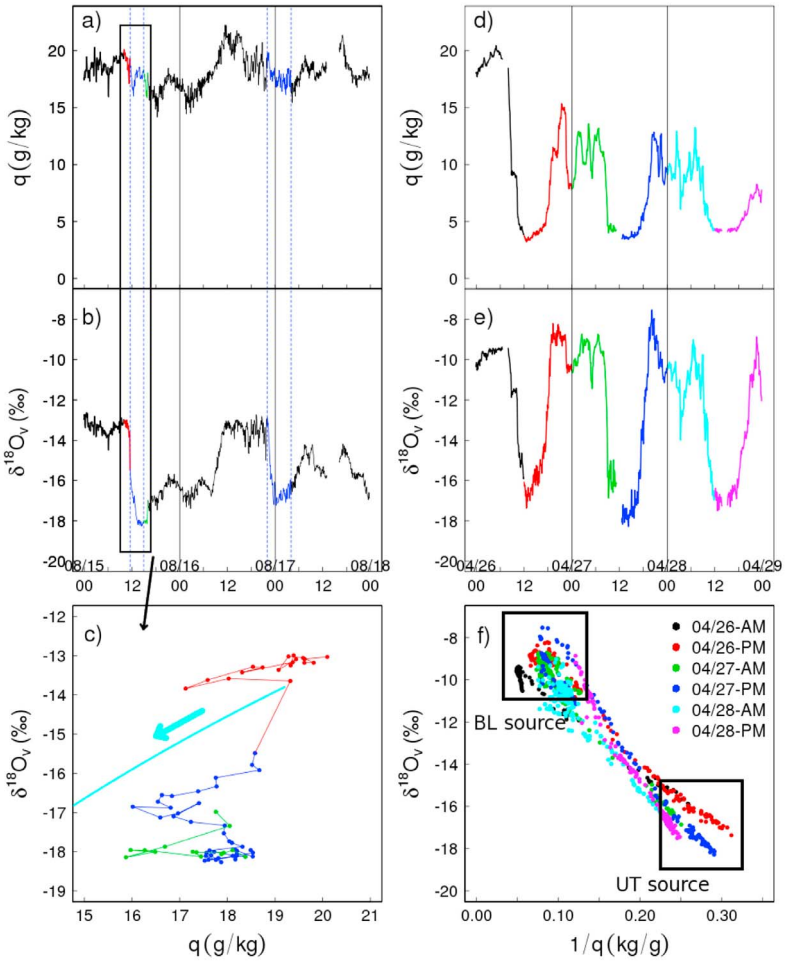

Figure 3. (a) Evolution of 5-min average q from 15 to 19 August 2011. (b) Same as Figure 3a but for $\delta^{18}O_v$. Blue dotted vertical lines correspond to the passage of meso-scale convective systems. The evolution of $\delta^{18}O_v$ for these events is representative of 84% of the sampled convective systems. (c) Relationship between δ^{18}Ov and q during 15 August 2011 (10UTC to 18UTC) where a meso-scale convective system brought 10.8 mm precipitation amount between 1130UTC and 1430UTC (blue dots). Cyan solid line accounts for a Rayleigh distillation under isotopic equilibrium conditions. We assume a condensation temperature of 0°C and an initial q ($\delta^{18}O_v$) of 19 g/kg (−13.8‰). (d) Same as Figure 3a but for 26 to 29 April 2011. (e) Same as Figure3b but for 26 to 29 April 2011. (f) Relationships between 5-min average $\delta^{18}O_v$ and 1/q over 12-h periods (am and pm) from 26 to 29 April 2011.

4.4. Diurnal Cycle During the Dry Season

[13] Outside of the monsoon season, a strong, repeatable diurnal signal is detected from November 2010 to May 2011. Specific humidity and $\delta^{18}O_v$ vary in phase (decreasing around 06–08 UTC to 12–14 UTC and increasing during the night) (Figures 3d and 3e). Maximum amplitudes are 10‰ (15 g/kg) peak to peak for $\delta^{18}O_v$ (q) and occur in April–May. A strong linear relationship between $\delta^{18}O_v$ and 1/q at a 12-hour scale is exhibited over this period (see Figure 3f) and reflects a mixing between two sources [*Noone et al.*, 2011], which are potentially the water vapor advected within the boundary layer during nighttime and the drier and more depleted water vapor from the free atmosphere entrained at the top of the boundary layer during daytime. Between 26 and 29 April 2011, where diurnal amplitudes are maximum, $\delta^{18}O_v$ of the boundary layer (upper tropospheric) source can be deduced from Figure 3f to be -8.62 ± 0.66‰ (-17.15 ± 0.79‰), n = 6. Thus, outside of the monsoon, $\delta^{18}O_v$ combined with q may be used to quantify the relative contribution of horizontal transport and convective mixing.

5. Comparison of Our Observations With LMDZ-iso

[14] Comparing our $\delta^{18}O_v$ observations to the nudged LMDZ-iso simulation [*Risi et al.*, 2010c] over 2010–2011 in the Niamey grid point, the model fails to reproduce the W-shape seasonal cycle and its amplitude (Figure 1c). The first isotopic depletion of low-level vapor observed from July to September 2010 is not as strong as in our observations ($\delta^{18}O_v$ is overestimated by 2.2‰) whereas on the opposite the model underestimates $\delta^{18}O_v$ during the dry season (by 4.6‰ in January). The model does not capture the intraseasonal variability of $\delta^{18}O_v$ during the monsoon season (σ_{obs} = 1.76‰ and σ_{LMDZ} = 0.66‰, calculated from daily averaged) (Figure 1c). However, from December 2010 to

May 2011, LMDZ-iso overestimates $\delta^{18}O_v$ variability (σ_{obs} = 2.16‰ and σ_{LMDZ} = 3.20‰). The LMDZ-iso hourly outputs are not available and prevent us from discussing the squall line scale.

6. Conclusion and Perspectives

[15] At the seasonal scale, $\delta^{18}O_v$ exhibits a "W-shape", different from the seasonality of the water vapor concentration. Our observations confirm the role of convective activity in depleting the low-level water vapor during the monsoon, and the depleting effect of large-scale subsidence north of 10°N during the dry season. At the intraseasonal scale, summer $\delta^{18}O_v$ records main modes likely associated to convection. Winter $\delta^{18}O_v$ is modulated by tropical/extra-tropical teleconnection through the propagation of a baroclinic wave train-like structure and intrusion of air originating from higher latitude. Winter diurnal cycle of $\delta^{18}O_v$ and q reflect boundary layer mixing process between the lower and upper atmosphere. During the monsoon season, the strongest diurnal variations are associated with rain events and may record the propagation of density currents. We show the potential of simultaneous q and $\delta^{18}O_v$ measurements to investigate the initiation of convection and to quantify convective processes such as meso-scale subsidence and rain evaporation within convective systems. Additional constraints will be brought by deuterium excess ($d = \delta D - 8\delta^{18}O$) on this aspect. Finally, we show that our observations are poorly reproduced by LMDZ-iso model and think that such in-situ time series can be very helpful for validating space-based remote sensing observations.

[16] **Acknowledgments.** We warmly thank J. R. Lawrence and M. Schneider for their very constructive and encouraging reviews. We thank G. Brissebrat, L. Fleury for their guidance to collect on-site meteorological data as well as J-P. Lafore, F. Guichard, F. Couvreux, D. Bouniol and R. Roehrig for fruitful discussions. We also thank V. Masson-Delmotte for her fruitful comments and Tahirou Bana Hachimou for on-site technical help. This work was funded by IRD and the INSU-LEFE-EVE YOUPI proposal.

[17] The Editor thanks James Lawrence and an anonymous reviewer for assisting with the evaluation of this paper.

References

Bony, S., C. Risi, and F. Vimeux (2008), Influence of convective processes on the isotopic composition ($\delta^{18}O$ and δD) of precipitation and water vapor in the tropics: 1. Radiative-convective equilibrium and Tropical Ocean–Global Atmosphere–Coupled Ocean-atmosphere Response Experiment (TOGA-COARE) simulations, *J. Geophys. Res.*, *113*, D19305, doi:10.1029/2008JD009942.

Chauvin, F., R. Roehrig, and J.-P. Lafore (2010), Intraseasonal variability of the Saharan heat low and its link with midlatitudes, *J. Clim.*, *23*, 2544–2561, doi:10.1175/2010JCLI3093.1.

Dansgaard, W. (1964), Stable isotopes in precipitation, *Tellus*, *16*, 436–468.

Frankenberg, C., et al. (2009), Dynamic processes governing lower-tropospheric HDO/H_2O ratios as observed from space and ground, *Science*, *325*, 1374–1377, doi:10.1126/science.1173791.

Gupta, P., D. Noone, J. Galewsky, C. Sweeney, and B. H. Vaughn (2009), Demonstration of high-precision continuous measurements of water vapor isotopologues in laboratory and remote field deployments using wavelength-scanned cavity ring-down spectroscopy (WS-CRDS) technology, *Rapid Commun. Mass Spectrom.*, *23*, 2534–2542.

Houze, R., S. Rutledge, M. Biggerstaff, and B. F. Smull (1989), Interpretation of Doppler weather-radar displays in midlatitude mesoscale convective systems, *Bull. Am. Meteorol. Soc.*, *70*, 608–619, doi:10.1175/1520-0477(1989)070<0608:IODWRD>2.0.CO;2.

Janicot, S., F. Mounier, S. Gervois, B. Sultan, and G. Kiladis (2010), The dynamics of the West African monsoon. Part V: The detection and role of the dominant modes of convectively coupled equatorial Rossby waves, *J. Clim.*, *23*, 4005–4024, doi:10.1175/2010JCLI3221.1.

Lafore, J.-P., C. Flamant, V. Giraud, F. Guichard, P. Knippertz, J.-F. Mahfouf, P. Mascart, and E. R. Williams (2010), Editorial introduction to the AMMA Special Issue on "Advances in understanding atmospheric processes over West Africa through the AMMA field campaign," *Q. J. R. Meteorol. Soc.*, *136*(S1), 2–7, doi:10.1002/qj.583.

Liebmann, B., and C. A. Smith (1996), Description of a complete (interpolated) outgoing longwave radiation dataset, *Bull. Am. Meteorol. Soc.*, *77*, 1275–1277.

Noone, N., et al. (2011), Properties of air mass mixing and humidity in the subtropics from measurements of the D/H isotope ratio of water vapor at the Mauna Loa Observatory, *J. Geophys. Res.*, *116*, D22113, doi:10.1029/2011JD015773.

Risi, C., S. Bony, F. Vimeux, L. Descroix, B. Ibrahim, E. Lebreton, I. Mamadou, and B. Sultan (2008a), What controls the isotopic composition of the African monsoon precipitation? Insights from event-based precipitation collected during the 2006 AMMA campaign, *Geophys. Res. Lett.*, *35*, L24808, doi:10.1029/2008GL035920.

Risi, C., S. Bony, and F. Vimeux (2008b), Influence of convective processes on the isotopic composition ($\delta^{18}O$ and δD) of precipitation and water vapor in the Tropics: 2. Physical interpretation of the amount effect, *J. Geophys. Res.*, *113*, D19306, doi:10.1029/2008JD009943.

Risi, C., S. Bony, F. Vimeux, C. Frankenberg, D. Noone, and J. Worden (2010a), Understanding the Sahelian water budget through the isotopic composition of water vapor and precipitation, *J. Geophys. Res.*, *115*, D24110, doi:10.1029/2010JD014690.

Risi, C., S. Bony, F. Vimeux, M. Chong, and L. Descroix (2010b), Evolution of the water stable isotopic composition of the rain sampled along Sahelian squall lines, *Q. J. R. Meteorol. Soc.*, *136*(S1), 227–242, doi:10.1002/qj.485.

Risi, C., S. Bony, F. Vimeux, and J. Jouzel (2010c), Water stable isotopes in the LMDZ4 general circulation model: Model evaluation for present day and past climates and applications to climatic interpretation of tropical isotopic records, *J. Geophys. Res.*, *115*, D12118, doi:10.1029/2009JD013255.

Stewart, M. K. (1975), Stable Isotope Fractionation Due to Evaporation and Isotopic Exchange of Falling Waterdrops: Applications to Atmospheric Processes and Evaporation of Lakes, *J. Geophys. Res.*, *80*(9), 1133–1146, doi:10.1029/JC080i009p01133.

Torrence, C., and G. Compo (1998), A practical guide to wavelet analysis, *Bull. Am. Meteorol. Soc.*, *79*, 61–78, doi:10.1175/1520-0477(1998)079<0061:APGTWA>2.0.CO;2.

Tremoy, G., F. Vimeux, O. Cattani, S. Mayaki, I. Souley, and G. Favreau (2011), Measurements of water vapor isotope ratios with wavelength scanned cavity ring-down spectroscopy technology: New insights and important caveats for deuterium excess measurements in tropical areas in comparison with isotope-ratio mass spectrometry, *Rapid Commun. Mass Spectrom.*, *25*, 3469–3480, doi:10.1002/rcm.5252.

O. Cattani, G. Tremoy, and F. Vimeux, Laboratoire des Sciences du Climat et de l'Environnement, UMR 8212, Institut Pierre Simon Laplace, CEA-CNRS-UVSQ, CE Saclay, Orme des Merisiers, Bât. 701, F-91191 Gif-sur-Yvette CEDEX, France. (guillaume.tremoy@lsce.ipsl.fr)

G. Favreau and M. Oi, Laboratoire HydroSciences Montpellier, UMR 5569, Institut de Recherche pour le Développement, CNRS-IRD-UM1-UM2, Place E Bataillon, F-34095 Montpellier CEDEX 5, France.

S. Mayaki and I. Souley, Institut des RadioIsotopes, Université Abdou Moumouni de Niamey, BP 10727, Niamey, Niger.

C. Risi, Laboratoire de Météorologie Dynamique, Institut Pierre Simon Laplace, UPMC-CNRS, 4 place Jussieu, F-75252 Paris CEDEX 05, France.